

# Evaluating Relay Beamwidth for Enhanced Coverage and Data Rates in Buoy-Assisted Maritime Communications

Kyeongjea Lee<sup>1</sup>, Tae -Woo Kim<sup>1</sup>, Sungyoon Cho<sup>2</sup>, Kiwon Kwon<sup>2</sup> and Dong Ku Kim<sup>1\*</sup>

<sup>1</sup> Department of Electrical engineering, Yonsei University Seoul, South Korea  
[e-mail: : kjlee92@yonsei.ac.kr, tw.kim@ yonsei.ac.kr, dkkim@yonsei.ac.kr]

<sup>2</sup> Smart Network Research Center, Korea Electronics Technology Institute Seoul, South Korea  
[e-mail: sycho@keti.re.kr, kwonkw@keti.re.kr]

\*Corresponding author: Dong Ku Kim

*Received March 31, 2023; revised February 21, 2024; accepted March 23, 2024;  
published April 30, 2024*

---

## Abstract

Maritime activities are on the rise, there is a growing demand for high-quality communication services that can cover larger areas. However, the transmission of high data rates to maritime users is challenging due to path loss from land base stations, which limits the transmission power. To overcome this challenge, researchers have been exploring the use of buoys in a marine environment as relays for communication technology. This paper proposes a simulation-based approach to investigate the impact of various beamwidths on communication performance when using a buoy as a relay. The objective is to determine the optimal beamwidth that yields the highest data rate for the target location. The approach is based on an offshore wave model where the direction of the buoy changes according to the height of the wave. The study investigates the performance of the relay in the downlink situation using receive beamforming, and the capacity at the user in the three-hop situation is verified using an amplify-and-forward (AF) relay that uses transmit beamforming to the user. The simulation results suggest that the beamwidth of the relay should be adjusted according to the wave conditions to optimize the data rate and relay position that satisfies a data rate superior to the direct path to the target position. Using a buoy as a relay can be a promising solution for enhancing maritime communications, and the simulation-based approach proposed in this paper can provide insights into how to optimize beamwidth for effective communication system design and implementation. In conclusion, the study results suggest that the use of buoys as relays for maritime communication is a feasible solution for expanding coverage and enhancing communication quality. The proposed simulation-based approach provides a useful tool for identifying relay beamwidths for achieving higher data rates in different wave conditions. These findings have significant implications for the design and deployment of communication systems in maritime environments.

---

**Keywords:** Maritime communication, ocean channel model, Extending Communication Coverage, Beamforming, AF relay

---

This research was a part of the project titled 'The advancement of smart aids to navigation facilities (20210636)', funded by the Ministry of Oceans and Fisheries, Korea.  
A preliminary version of this paper was presented at ICONI 2022.

## 1. Introduction

Maritime communication plays a crucial role in ensuring the safety, security, and efficiency of various ocean-based activities, including shipping, offshore energy production, and environmental monitoring [1]. However, conventional maritime communication systems face challenges such as limited coverage and signal degradation due to the unique characteristics of the marine environment, including the Earth's curvature, atmospheric and sea state variations, and interference from other communication systems. With the increasing reliance on maritime activities, the need for reliable and affordable communication systems has become crucial. Ensuring the safety of navigation and providing infotainment services to seafarers is crucial for the smooth running of maritime activities. The establishment of maritime communication systems has been the focus of many initiatives aimed at improving the quality and coverage of communication services [2],[3]. And various researchers have explored the use of navigational aids as relay nodes to extend communication coverage and improve the performance of maritime communication networks [5]. This approach not only enhances the coverage area but also increases the reliability and robustness of the communication system. Existing marine communication systems primarily rely on satellite and very-high frequency VHF communication [6]. For example, the International Maritime Satellite System (INMARSAT) [7] has been developed to provide high-speed communication in oceans. However, conventional maritime VHF communication systems are limited in their ability to support high data rate multimedia services due to their limited bandwidth. Developing new technologies that can provide low-cost, high-rate multimedia information services in maritime environments remains an area of active research. One such technology that has been widely used to extend coverage and improve spatial diversity gain in terrestrial broadband communication systems is relay-aided communication [7]. Relay communication technology has also been extended to marine scenarios to support efficient and reliable information services. For instance, Zhou et al. constructed a multi-hop ship-to-shore wireless mesh network that relied on ships and buoys acting as relay nodes, achieving a coverage of 30 km at 6 Mbps [8]. In this thesis, we propose a relay-aided MIMO communication system using buoys as relay nodes to enhance maritime communication systems. The primary objective of the proposed system is to identify optimal relay locations that offer a superior data rate compared to the direct path between the transmitter and the target location, as well as to select the optimal beamwidth for the antenna based on its height and prevailing wave conditions. The system's performance is evaluated through capacity measurements, which serve as a key indicator of its effectiveness in various scenarios. To achieve this objective, we present an Amplify-and-Forward (AF) relay protocol that improves the system's capacity. The system employs a simulation-based approach, leveraging advanced algorithms and computational techniques to model the complex interactions between these factors and their impact on communication capacity. By conducting extensive simulations, the system can identify relay locations that consistently provide higher data rates than the direct path to the target location, accounting for variations in antenna height and wave conditions. Furthermore, the proposed system examines the effects of different beamwidths on communication performance,

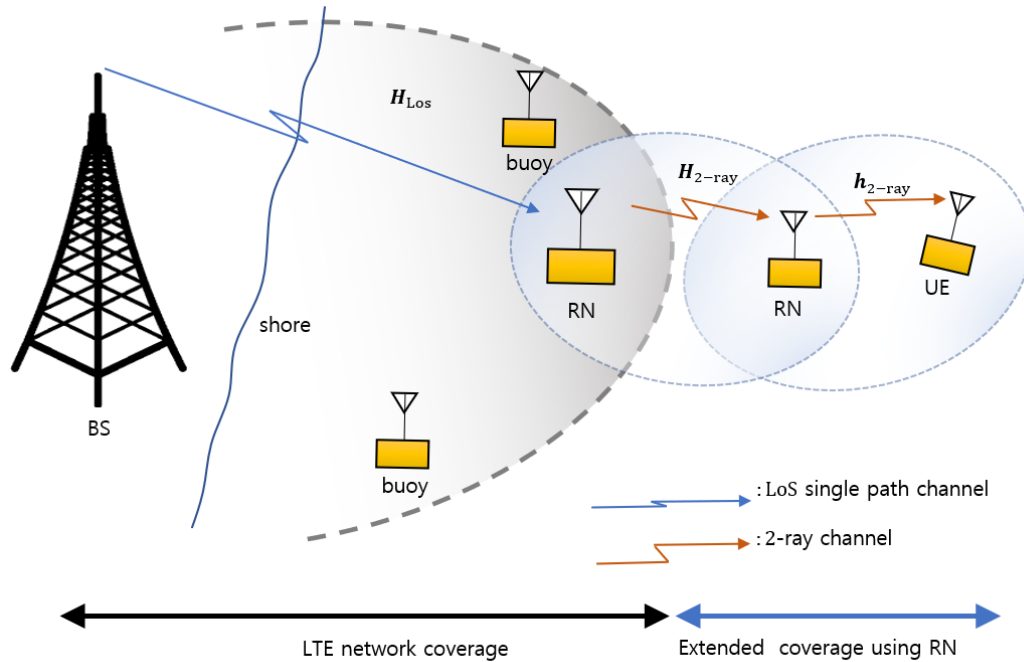


**Fig. 1.** System architecture in maritime communication

enabling the selection of the optimal beamwidth for each relay location. This analysis considers the trade-offs between narrower and wider beamwidths, considering factors such as signal strength, interference, and coverage area. In Section 2 of this thesis, we elaborate on the channel model for the proposed relay-aided MIMO communication system using buoys. In Section 3, we present the continuous Line-of-sight (CLOS) as a function of wave height and antenna height. In Section 4, we present the AF relay protocol and explain how it can improve the system's capacity. We then conduct numerical simulations in Section 5 to evaluate the performance of the proposed system under different scenarios. Finally, we summarize the findings of this thesis in Section 6 and suggest avenues for future research. Overall, the proposed relay-aided MIMO communication system using buoys has the potential to enhance maritime communication systems' reliability and affordability, supporting the growing demand for communication services in maritime activities.

## 2. Channel Model

The near-shore communication channel, which extends from a cellular tower to ships, experiences less reflection from the ocean surface, making the line-of-sight (LOS) path more prominent. Conversely, the second hop in the offshore communication channel may face significant reflection from the sea surface, potentially leading to serious multipath effects. Therefore, in our model, Line-of-sight (LoS) single path is conceived for describing the first hop near-shore channel. Additionally, a modified two-ray reflection model is employed to describe the second off-shore channel.

In the paper the scenario depicted in **Fig. 1**, which involves using buoys as relay nodes in a linear topology for maritime communications, is both practical and valid for several reasons. Firstly, the linear topology, where only adjacent nodes can communicate, mirrors realistic

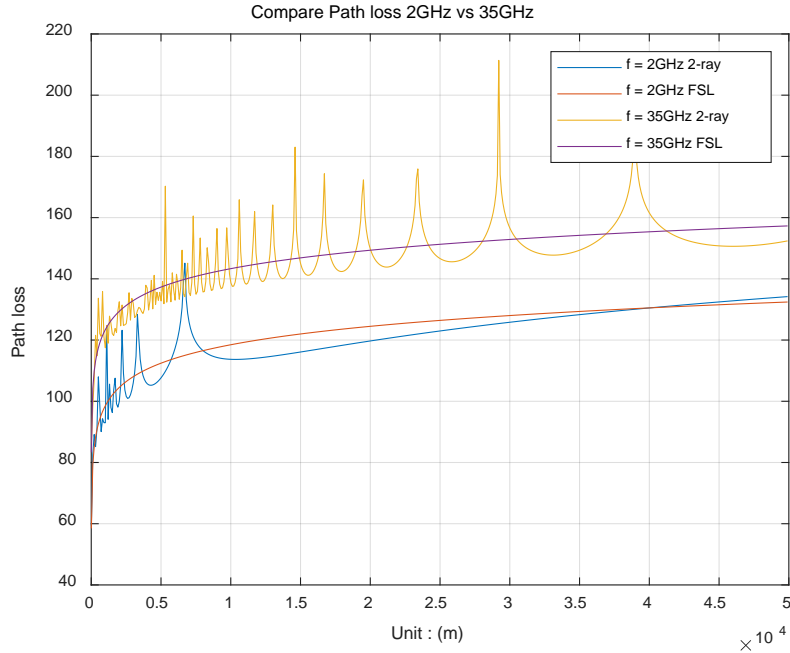


**Fig. 2.** The Path loss results using the FSL, 2-ray.

maritime environments where direct communication lines between source and destination are often not feasible due to distance, obstacles, or other environmental factors. In such scenarios, utilizing buoys as relay stations is a practical solution to enhance signal strength and coverage over large maritime areas.

Secondly, the assumption of complete Channel State Information (CSI) availability to both the source and destination is a common theoretical simplification that aids in focusing on the core aspects of the proposed system, such as the impact of relay beam width on communication efficacy. While in real-world applications, considering Imperfect Channel State Information (ICSI) is crucial for a more accurate representation, the exclusion of ICSI in this theoretical model is valid for the purpose of evaluating the primary effects of relay beam width and positioning. Therefore, despite some simplifications, the scenario in **Fig. 1** provides a relevant and feasible framework for studying and enhancing maritime communication systems using buoy-assisted relays.

## 2.1 Direct path channel model

We assume that the distance between the base station to the relay and the destination is so far that the characteristics of the 2-ray channel [9] is approximated to the Line-of-Sight (LoS) characteristics [10].

$$PL_{LoS} = -27.56 + 20 \log_{10}(d) + \log_{10}(f) \quad (1)$$

## 2.2 2-ray path channel model

Due to the characteristics of ocean surface, the two-path model including a direct beam from the relay to the receiver and a reflected beam at sea level is widely used in ocean channel

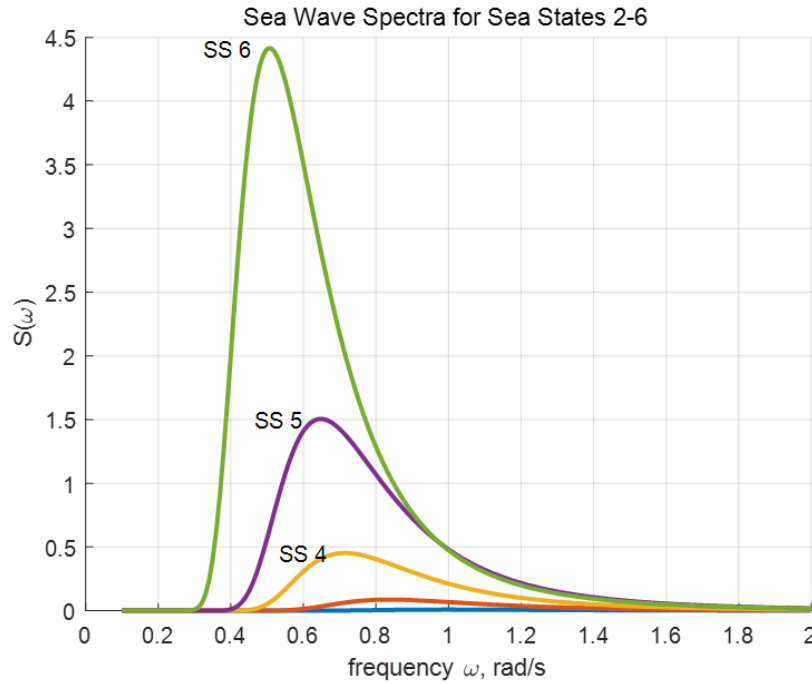


**Fig. 3.** Bretschneider sea wave spectral model for sea state 2-6

model [10]. In simulations, we assume that wind speeds are experiencing calm conditions in the sea where they are not high enough to change the roughness of radio wave significantly. In coastal scenarios, we assume that the sea level is flat and that there are few large waves that cause roughness. In this paper, for simplicity, the roughness of the sea level was regarded as 0, and the reflection coefficient was assumed to be -1 [11].

$$PL_2 = -20 \log_{10} \left\{ \left( \frac{\lambda}{4\pi d} \right) \left| 1 + \text{Re} \exp \left( \frac{j\alpha 2\pi \Delta d}{\lambda} \right) \right| \right\} \quad (2)$$

The free space path loss and 2-ray path mentioned above appear in **Fig. 2**, depending on the distance for each frequency.

### 2.3 Buoy angle

In this paper, we use the Bretschneider spectral model [12],[13], also known as the ISSC spectrum, for wave modeling in inland seas. It is a statistical model that uses a combination of wind speed and direction to estimate the significant wave height and spectral energy density. The model assumes that waves in the ocean are random and that the energy of the waves is distributed across different frequencies and spectral model is illustrated in **Fig. 3**. The Bretschneider model is widely used in ocean engineering and offshore structures design to estimate the wave loads and responses of structures.

#### 2.3.1 Bretschneider Spectral Model

$$S_\gamma(\omega) = \frac{5}{16} \frac{H_s^2 \omega_p^4}{\omega^5} \exp \left( -\frac{5}{4} \left( \frac{\omega_p}{\omega} \right)^4 \right) \quad m^2 / (rad/s) \quad (3)$$

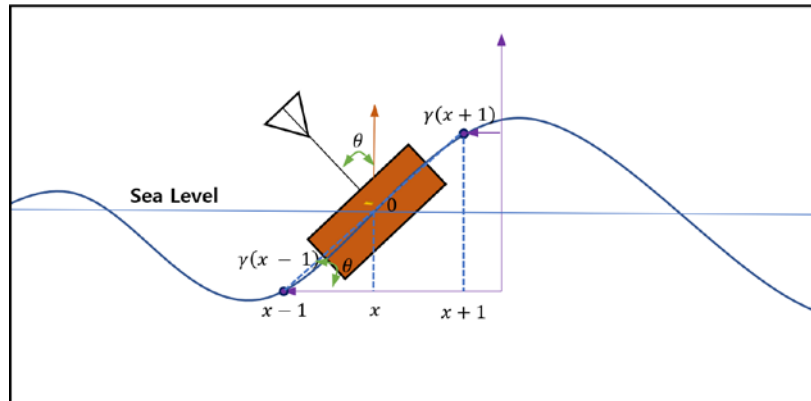


**Fig. 4.** Modeling the angle of a buoy in a dynamic ocean environment.

In the spectral model expressed as (3),  $H_s$ ,  $\omega_p$  represent the height (m) of the wave and peak angular frequency (rad/s), respectively. Here, peak period is  $T_p = 2\pi/\omega_p$ .

### 2.3.2 Modeling the height of the sea level

The actual wave consists of a large number of frequencies ( $N_f$ ). Therefore, the wave is the sum of all frequency elements as shown in (4)[12].

$$\gamma(x, t) = \sum_{i=1}^{N_f} a_i \cos(2\pi f_i t + k_i x + \alpha_i) \quad (4)$$

where  $a_i$ ,  $k_i = w_i^2/g$ ,  $\alpha_i$  are amplitude, wave number, and phase for the  $i$ -th frequency  $f_i$ , respectively. Furthermore, the expected amplitude  $\mu_i$  of each frequency component can be calculated as [14]

$$\mu_i = \sqrt{2 * S_\gamma(\omega_i) * \Delta\omega} \quad (5)$$

$\Delta\omega$  is the frequency interval of the spectrum  $S_\eta(\omega_i)$ . Amplitude ( $a_i$ ) is obtained by returning the values calculated using (5) to values following the Rayleigh distribution [15].

### 2.3.3 Modeling the angle of buoy

The angle  $\theta$  between the antenna and the sea level is an important parameter in our study of ocean waves and their impact on structures. As this angle is continuously changing over time, it is necessary to develop an approach to estimate its value. To accomplish this, we utilize the method illustrated in Fig. 4, which involves drawing an auxiliary tangent across point O at a horizontal coordinate  $x$  in meters. This tangent is perpendicular to the vertical line of the sea level, and the resulting angle  $\theta$  can be approximated using (6)

$$\theta = \tan^{-1} \left( \frac{\gamma(x+1) - \gamma(x-1)}{2} \right) \quad (6)$$

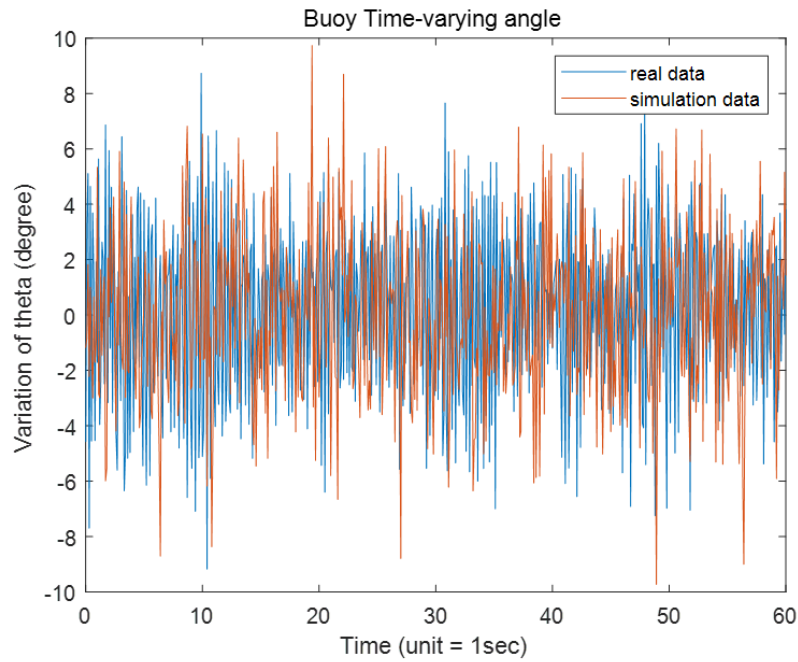


**Fig. 5.**  $\theta$  variation over time for the ocean wave combination (Sea state level 4)

where  $\gamma(x)$  represents the surface elevation. This equation involves calculating the surface elevation  $\gamma(x)$  at point O and taking the difference in elevation between the points to the left and right of O, which are  $x-1$  and  $x+1$ , respectively. By averaging these differences and applying a tangent function, we obtain an estimated value of  $\theta$ . This approach provides a means to track the changes in the angle over time, enabling us to gain insights into the behavior of ocean waves. To gain a comprehensive understanding of the behavior of ocean waves, it is essential to examine the variation of the angle  $\theta$  over time, which represents the slope of the tangent between the antenna and the sea level. To validate the accuracy of the estimated  $\theta$ , actual measurement data from a gyro sensor installed on a buoy floating in the sea is utilized. The actual measured values of the angle of the buoy movement indicate that the average angle is 0.4 degree and the variance is 8.8 degree. Through mathematical modeling for a moderate sea state level, the average movement angle of the buoy is about 0.3 degree and the variance is about 8.9 degree. Then, it is depicted in Fig. 5. Mathematical modeling of the moving angle of the buoy is used to construct a time-varying channel. The accuracy and reliability of the modeled channel were verified by comparing it with the channel model based on the actual data.

### 3. Probability of Continuous LoS Duration

In this section, it is crucial to determine the obstruction of the line-of-sight (LoS) between a base station and a buoy within a specific distance. To accomplish this, we utilize (4), which involves calculating the ratio of the angles formed between the base station and the buoy, and between the base station and the point at which the signal is obstructed by waves. This equation provides a means to estimate the LoS obstruction by considering the angles formed by the signal and the obstruction caused by waves. By analyzing this obstruction, we can gain insights

into the behavior of wireless signals in the presence of ocean waves, which is critical for designing effective wireless communication systems for marine applications. The results of

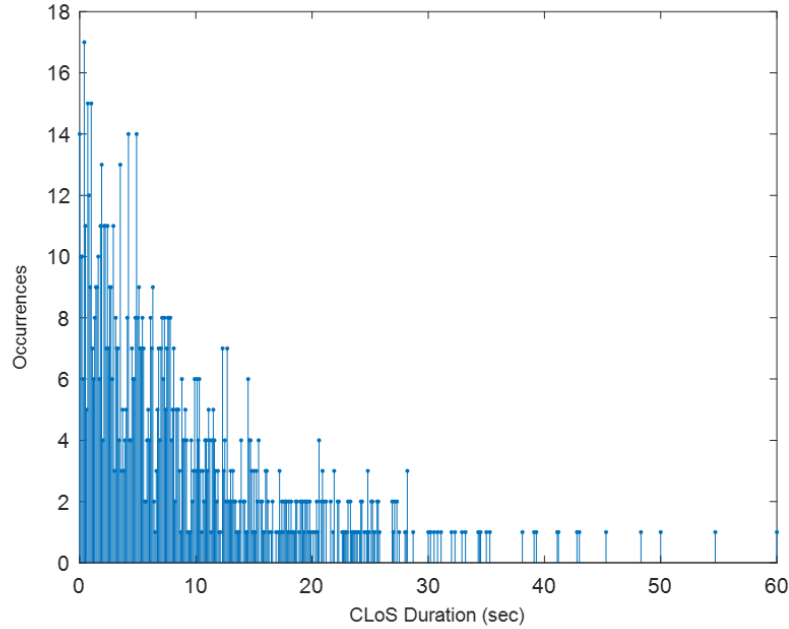


**Fig. 6.** Occurrence of the continuous LoS duration for moderate sea state (antenna height = 1m)

this analysis can be used to optimize the placement of antennas and other communication equipment, ensuring reliable communication between offshore structures and shore-based facilities.

$$\frac{h_{tw} - (\gamma(0, t) + h_a)}{d} > \frac{h_{tw} - \gamma(x_n, t)}{d - x_n} \quad (7)$$

In this equation,  $h_{tw}$  represents the height of the base station,  $h_a$  represents the height of the buoy's antenna,  $d$  represents the distance between the buoy and the base station,  $x_n$  represents an arbitrary position between the buoy and the base station, and  $\eta$  represents the height of the sea level. The left-hand side of the equation indicates the point where the obstruction of the LoS is most likely to occur, as it represents the larger value. And we can assume that buoy antenna and buoy are located at the same horizontal origin. It is summarized in [16], which finds the nearest ocean wave breaker(s) and analyzes the average LoS probabilities and stochastic continuous LoS segments. Our method utilizes continuous LoS (CLoS) and continuous blocked LoS (BLOS) segments to determine the total LoS time duration and probability of LoS communication. Within  $T$  second window, we define CLoS segments with time intervals  $t_1, t_2, \dots, t_n$ . The total LoS time duration is denoted as  $T_{LoS} = \sum_{n=1}^N t_n$ . The probability of LoS communication,  $P_{LoS}$  is calculated by

$$P_{LoS} = \frac{T_{LoS}}{T} = \frac{\sum_{n=1}^N t_n}{T} \quad (8)$$



and  $P_{BLoS} = 1 - P_{LoS}$ . In the simulation, as shown in (8), it was assumed that the link of the signal was broken when a blockage point occurred due to waves. **Fig. 6, 7** are simulation results for CLoS according to antenna height in the case of moderate waves.

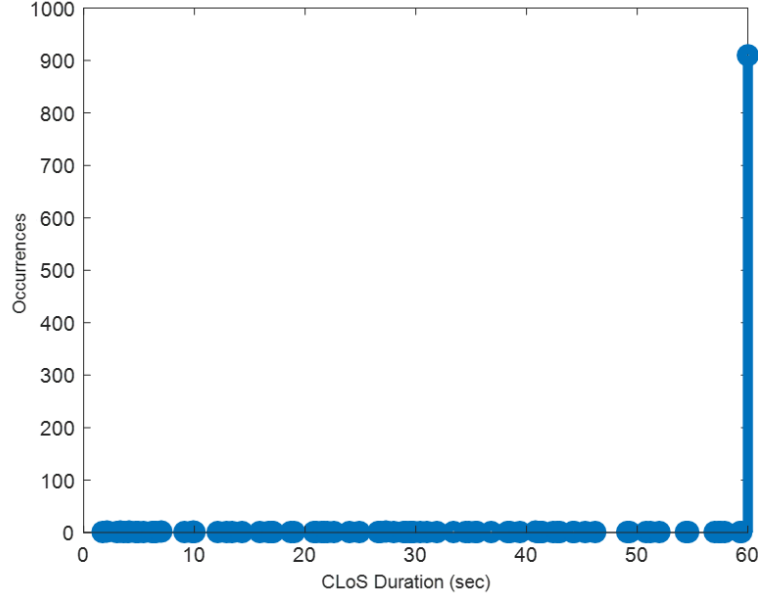


**Fig. 7.** Occurrence of the continuous LoS duration for moderate sea state (antenna height = 3m)

#### 4. Amplify and Forward relay process

In this work, we consider a three-hop relay channel where the source (Base Station, BS), a full-duplex relay node (RN) with multiple antennas, and the destination (User Equipment, UE) with a single antenna are involved, as depicted in **Fig. 1**. Throughout the paper, we assume that the channel is arranged in a linear topology. This implies that only adjacent nodes can “see” and communicating with each other, as described in [17]. Consequently, there is no direct link between the source and destination, and each node relies on the relay node to facilitate communication and the full CSI is available to the source and destination. We focused on evaluating the performance of the modeled channel environment and therefore ignored the imperfect channel state information (ICSI) in our analysis. Therefore, the signal received by relay is

$$\mathbf{Y}_{rel} = \mathbf{F}_r \mathbf{H}_{LoS} \mathbf{x} + \boldsymbol{\xi}_{LoS} \quad (9)$$

where  $\mathbf{x}$  is the signal transmitted by BS,  $\mathbf{H}_{LoS}$  is the first hop channel between BS and relay,  $\mathbf{F}_{r_i}$  is the  $i$ -th relay’s receive beamforming matrix and  $\boldsymbol{\xi}_{LoS} \sim \mathcal{CN}(\mathbf{0}, \sigma_{rel}^2 \mathbf{I})$  is additive white Gaussian noise (AWGN) processes at relay and  $\mathbf{I}$  is an identity matrix. The signal transmitted by the relay in the AF mode is  $\sqrt{K} \mathbf{Y}_{rel}$ , where  $K$  is its power gain. Thus, the input-output relationship of the whole three-hop AF relay channel is [18]

$$\mathbf{y}_{UE} = \sqrt{K_2 * K_1} \mathbf{h}_{2\text{-ray}} \mathbf{F}_{r_2} \mathbf{H}_{2\text{ray}} \mathbf{F}_{r_1} \mathbf{H}_{\text{LoS}}^+ \mathbf{x} + \sqrt{K_2 * K_1} \mathbf{h}_{2\text{-ray}} \mathbf{F}_{r_2} \mathbf{H}_{2\text{ray}} \boldsymbol{\xi}_{r_1} + \sqrt{K_2} \mathbf{h}_{2\text{ray}} \boldsymbol{\xi}_{r_2} + \boldsymbol{\xi}_{UE} \quad (10)$$

where  $\mathbf{h}_{2\text{-ray}}$  third hop channel between relay and user,  $\mathbf{y}_{UE}$  is a received signal at UE,  $\boldsymbol{\xi}_{r_i} \sim \mathcal{CN}(\mathbf{0}, \sigma_{r_i}^2)$  and  $\boldsymbol{\xi}_{UE} \sim \mathcal{CN}(\mathbf{0}, \sigma_{UE}^2)$  are additive white Gaussian noise (AWGN) at relay and user, respectively.  $^+$  denotes Hermitian conjugation. To find the SNR at the destination in (11) can be expressed as

$$\gamma_{AF} = \frac{K_2 * K_1 g_3 \mathbf{F}_{r_2} g_2 \mathbf{F}_{r_1} \mathbf{H}_{\text{LoS}}^+ \mathbf{R}_x \mathbf{H}_{\text{LoS}}}{\sigma_D^2} \quad (11)$$

Where  $\mathbf{R}_x = E\{xx^+\}$  is the covariance matrix of the source transmitted signal,  $g_2 = |\mathbf{H}_{2\text{-ray}}|^2$  is the power gain of the second hop channel, and  $\sigma_D^2 = \sigma_{UE}^2 + \mathbf{F}_{r_1} \mathbf{F}_{r_2} \sum_{i=1}^2 \sigma_{r_i}^2 \sqrt{K} \prod_{i=2}^3 g_k$  is the total noise power at the destination. The AF relay capacity error-free data transmission in the AF protocol, can now be succinctly expressed in (11) as

$$C_{AF} = \log(1 + \gamma_{AF}) [\text{bps/Hz}] \quad (12)$$

The capacity at the destination is obtained by setting the relay positions differently through the following capacity (12).

## 5. Simulation

In Section 5, we provide a more comprehensive explanation of the simulation methodology to demonstrate its validity and relevance in evaluating the performance of the maritime communication system. This section outlines the detailed steps and rationale behind our simulation approach, focusing on how we model the maritime environment and the relay network. Firstly, we elaborate on the selection of the three-hop AF relay network configuration, as illustrated in [Fig. 1](#), highlighting why this setup is particularly suitable for maritime communication. We detail the reasons for equipping the base station (BS) and relays with four antennas, and the user equipment (UE) with a single antenna, emphasizing how this mirrors real-world maritime communication systems. Next, we delve into the channel modeling, explaining our rationale for assuming a LoS single path channel for the first hop (BS to relay) and a 2-ray channel for the subsequent hops. This part of the section includes a discussion on how these models accurately represent the signal propagation over water and the specific challenges posed by the maritime environment, such as wave movement and path loss. We include a detailed description of how we incorporated the angle of the buoy and path loss into our channel model to ensure it reflects the dynamic nature of maritime environments. Furthermore, we expand on the system parameters summarized in [Table 1](#), providing a detailed justification for each parameter choice and how they impact the simulation results.

**Table 1.** Applications in each class

Parameters	Values
Center Frequency	2 GHz
Bandwidth	10 MHz
BS antenna Height	30 m
Relay antenna height	2, 3 m

UE antenna height	5 m
Beamwidth	15°, 30°, 45°
BS power	46 dBm
Relay power	23 dBm
Sea state level	Level 2,3,4,5,6
Ocean wave period	10 sec
Distance BS – Relay1	10 km
Distance Relay1 – Relay2 – UE	5 km

This is followed by an in-depth analysis of the results depicted in [Fig. 8](#), explaining how the different distance ratios among the hops (BS-relay, relay-relay, relay-destination) were chosen and their significance in the study. Additionally, we provide a thorough explanation of the results obtained from varying the relay's beam width, as shown in [Fig. 9](#) and [Fig. 10](#). This includes a discussion on how different beam widths affect the receive beam gain and the system's overall capacity, particularly under varying sea state levels. By enhancing Section 5 with these additional details, we aim to clarify the robustness and relevance of our simulation methodology, ensuring that the reader can fully appreciate the depth and accuracy of our approach in modeling and evaluating maritime communication systems. To verify the practical validity, we explain the simulation parameter settings. The simulation uses a center frequency of 2 GHz with a bandwidth of 10 MHz. This choice is consistent with typical frequencies used in maritime communications, particularly in LTE (Long-Term Evolution) systems. The 2 GHz band is commonly used for mobile communications and is suitable for maritime environments where high data rate transmission is required over water. The base station (BS) antenna height is set at 30 meters, the relay antenna heights vary between 2 to 3 meters, and the user equipment (UE) antenna height is 5 meters. These heights are realistic for maritime communication setups, considering the elevated position of base stations on land and the lower height of antennas on buoys and ships. The beam widths used in the simulation (15°, 30°, 45°) allow for a detailed analysis of different focusing levels of the transmitted signal, which is crucial in understanding how beam width impacts signal coverage and quality in maritime environments. The BS power is set at 46 dBm and the relay power at 23 dBm. These power levels are representative of real-world base stations and relay nodes, ensuring that the simulation reflects actual maritime communication power constraints. The simulation incorporates varying sea state levels (levels 2 to 6) and an ocean wave period of 10 seconds. These parameters are critical in assessing the performance of the communication system under different marine conditions. The chosen sea state levels and wave period provide a comprehensive range of scenarios, from calm to moderately rough sea conditions, affecting the buoy's movement and, consequently, the communication link's stability. The distances set in the simulation, such as 10 km from the BS to the first relay and 5 km between subsequent relays and the UE, are typical of maritime scenarios where long-range communication is necessary due to the vastness of marine environments. Overall, the parameter settings in the simulation are well-justified and align with the conditions and requirements of maritime communications. They reflect a realistic setup for analyzing the impact of various factors, such as relay beam width and sea state, on the performance of buoy-assisted maritime communication systems. The simulation model is designed to reflect the unique challenges of maritime communication, accounting for the specific environmental conditions encountered at ocean. A critical aspect of the simulation is the channel modeling. The first hop, from the BS to the relay, is considered as a direct Line-of-Sight (LoS) single path channel, mirroring the relatively clear line of sight typically available in maritime settings. In contrast, the second and third hops, between relays and from relay to destination, are modeled as 2-ray channels. This distinction is crucial as it realistically

captures the complexity of signal propagation over water, particularly influenced by factors such as wave movement, sea state, and other maritime conditions. Additionally, the simulation pays special attention to environmental variables like the angle of the buoy and path loss. By incorporating these factors, the study provides a more nuanced understanding of how signals behave in maritime environments, which can vary significantly from terrestrial settings.

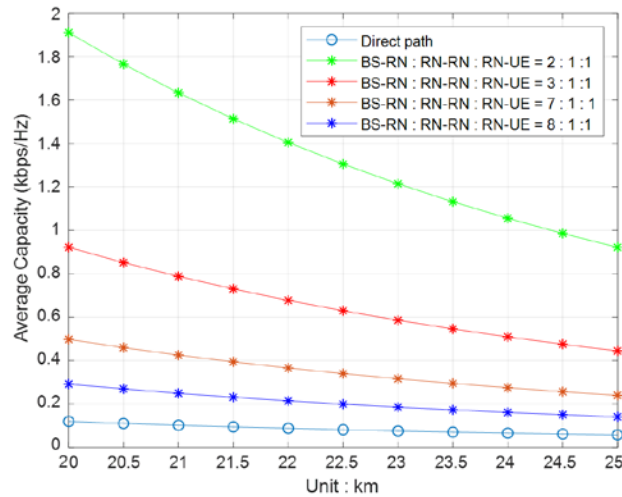


**Fig. 8.** Capacity performance according to the relay position

The angle of the buoy, for instance, can have a substantial impact on signal strength and quality, especially in rough sea conditions. The relay system's performance is examined under various configurations and distance ratios among the three hops (BS-relay, relay-relay, and relay-destination). These ratios include 2:1:1, 3:1:1, 7:1:1, and 8:1:1, offering insights into how the physical placement of relays affects the overall network efficiency as depicted **Fig. 8**. Such analysis is vital for practical deployment strategies in real-world maritime communication scenarios. Additionally, **Fig. 9** is simulated the impact of ocean waves on the beamforming gain in a maritime communication system. It calculates the movement and angle change of a buoy's antenna due to waves, and analyzes the beamforming gains for different antenna configurations. This is a histogram showing the distribution of beamforming gains for beam width of 30 degrees, illustrating the variability of gains due to the wave-induced motion. Furthermore, the study explores the implications of varying beam width at the relay, assessing how different degrees of beam width (15, 30, and 45 degrees) influence the network's capacity as depicted **Fig. 10**. This analysis is particularly significant as it demonstrates that the optimal beam width can vary depending on the sea state level. Narrower beam widths tend to be more effective in calmer sea conditions, enhancing signal focus and reducing interference. Conversely, in rougher sea states, a wider beam width helps maintain communication by covering a larger area, countering the effects of signal scattering due to waves and movement. In conclusion, the methodology adopted in this study is comprehensive, effectively capturing the intricate aspects of maritime communications. It not only considers the environmental dynamics unique to maritime settings but also examines the strategic placement of relay stations and the technical nuances of beam width adjustments. This thorough approach enables the evaluation of buoy-assisted maritime communication systems' performance, providing valuable insights for enhancing system design, improving energy efficiency, and ensuring robust signal coverage in various maritime scenarios. The detailed analysis offers a significant

contribution to the field, showcasing how advanced simulation techniques can be employed to optimize communication systems in challenging maritime environments.

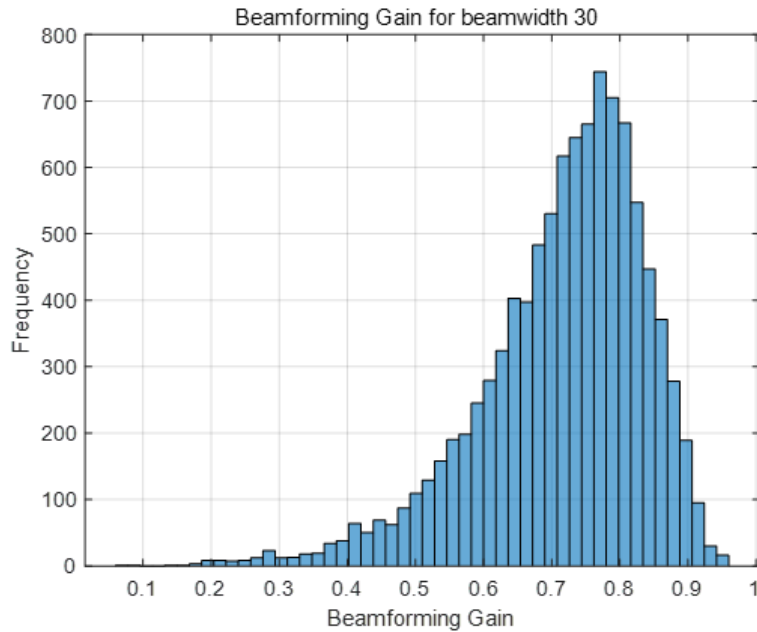


**Fig. 9.** Beam gain according to moderate sea state (Beam width = 30 degree)

## 6. Conclusion

In this paper, the methodology adopted in the paper to model the channel and evaluate its performance. One of the key strengths of this approach is that it takes into account the effect of sea state level on the channel, which is an important consideration for wireless communication in maritime environments. We first conducted mathematical modeling of the ocean wave elevation using the Bretschneider spectral model and then using this determined angle of the buoy. Taking into account the aforementioned considerations, we performed time-varying channel modeling and validated it using actual measurement data. In this channel model, we also estimate the obstruction of the LoS (Line of Sight) caused by ocean waves. By analyzing the angles formed by the signal and the obstruction caused by waves, insights can be gained into the behavior of wireless signals in marine environments. This information is crucial for designing effective wireless communication systems for marine applications. The results of this analysis can be used to optimize the placement of antennas and other communication equipment, ensuring reliable communication between offshore structures and shore-based facilities. Considering overall mentioned, we compared the capacity with respect to target location and beamwidth of the relay, especially in the context of the three-hop AF relay, allows for a thorough evaluation of the performance of the channel model. By using an appropriate beamwidth depending on the sea state, it is possible to achieve higher capacity with the same power in near-shore communication systems. This result means that energy efficiency can be obtained by utilizing adaptive beamforming techniques to adjust the beamwidth according to the sea state. Specifically, even with reduced power consumption, the system can maintain the same level of capacity by adjusting the beamwidth. Therefore, our

study highlights the potential for achieving energy efficiency in near-shore communication systems by optimizing the beamwidth. Overall, the simulation results provide valuable insights into the performance of the channel in different sea state conditions and can be used to optimize communication systems for maritime environments. This approach can be particularly useful for designing reliable and efficient communication networks for various maritime applications, such as offshore drilling, maritime surveillance, and maritime transportation. The exploration of novel techniques in this domain will significantly contribute to the advancement and robustness of the proposed communication framework for oceanic channels.

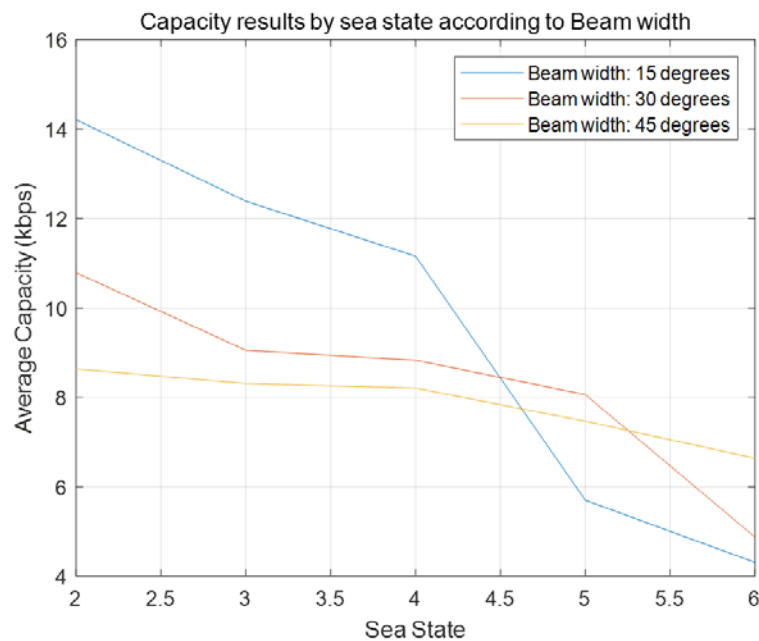


**Fig. 10.** Capacity performance according to sea state (Beam width = 15,30,45 degree)

## References

- [1] A. Zolich et al., "Survey on communication and networks for autonomous marine systems," *J. Intell. Robot. Syst.*, vol. 95, no. 3, pp. 789–813, April. 2019. [Article \(CrossRef Link\)](#)
- [2] D. Palma, "Enabling the Maritime Internet of Things: CoAP and 6LoWPAN Performance Over VHF Links," *IEEE Internet of Things Journal*, vol. 5, no. 6, pp. 5205-5212, Dec. 2018. [Article \(CrossRef Link\)](#)
- [3] T. Yang, Z. Zheng, H. Liang, R. Deng, N. Cheng and X. Shen, "Green Energy and Content-Aware Data Transmissions in Maritime Wireless Communication Networks," *IEEE Transactions on Intelligent Transportation Systems*, vol. 16, no. 2, pp. 751-762, April. 2015. [Article \(CrossRef Link\)](#)
- [4] S. Li, W. Qu, C. Liu, T. Qiu, and Z. Zhao, "Survey on high reliability wireless communication for underwater sensor networks," *J. Netw. Comput. Appl.*, vol. 148, no. 3, Dec. 2019. [Article \(CrossRef Link\)](#)
- [5] D. Kidston and T. Kunz, "Challenges and opportunities in managing maritime networks," *IEEE Communications Magazine*, vol. 46, no. 10, pp. 162-168, Oct. 2008. [Article \(CrossRef Link\)](#)
- [6] J. G. Puente, "The emergence of commercial digital satellite communications," *IEEE Communications Magazine*, vol. 48, no. 7, pp. 16-20, July. 2010. [Article \(CrossRef Link\)](#)

- [7] Y. Yang, H. Hu, J. Xu and G. Mao, "Relay technologies for WiMax and LTE-advanced mobile systems," *IEEE Communications Magazine*, vol. 47, no. 10, pp. 100-105, Oct. 2009. [Article \(CrossRef Link\)](#)
- [8] M. -t. Zhou et al., "TRITON: high-speed maritime wireless mesh network," *IEEE Wireless Communications*, vol. 20, no. 5, pp. 134-142, Oct. 2013. [Article \(CrossRef Link\)](#)
- [9] T. Wei, W. Feng, Y. Chen, C. -X. Wang, N. Ge and J. Lu, "Hybrid Satellite-Terrestrial Communication Networks for the Maritime Internet of Things: Key Technologies, Opportunities, and Challenges," *IEEE Internet of Things Journal*, vol. 8, no. 11, pp. 8910-8934, June. 2021. [Article \(CrossRef Link\)](#)
- [10] N. Mehrnia and M. K. Ozdemir, "Novel maritime channel models for millimeter radiowaves," in *Proc. of 2016 24th International Conference on Software, Telecommunications and Computer Networks (SoftCOM)*, pp. 1-6, 2016. [Article \(CrossRef Link\)](#)
- [11] H. -J. Kim, J. -K. Choi, D. -S. Yoo, B. -T. Jang and K. -T. Chong, "Implementation of MariComm bridge for LTE-WLAN maritime heterogeneous relay network," in *Proc. of 2015 17th International Conference on Advanced Communication Technology (ICACT)*, pp. 230-234, July 2015. [Article \(CrossRef Link\)](#)
- [12] L. H. Holthuijsen, *Waves in Oceanic and Coastal Waters*, Cambridge U.K.: Cambridge Univ. Press, 2007, pp. 15-50. [Article \(CrossRef Link\)](#)
- [13] J. Prendergast, M. Li and W. Sheng, "A Study on the Effects of Wave Spectra on Wave Energy Conversions," *IEEE Journal of Oceanic Engineering*, vol. 45, no. 1, pp. 271-283, Jan. 2020. [Article \(CrossRef Link\)](#)
- [14] S. J. Beatty, C. Hiles, B. Bocking, "Validation of a compact wave measurement buoy with rotational motion tests and field measurements off the Pacific Coast of British Columbia, Canada," *MarineLabs*, Aug. 2018. [Online]. Available: <https://www.aanderaa.com/media/pdfs/data-validation-motus-wave-buoys-wp002.pdf>
- [15] S. -W. Seo, K. -H. Shin, M. -M. Koo, K. Hong, I. -J. Yoon and J. -Y. Choi, "Experimentally Verifying the Generation Characteristics of a Double-Sided Linear Permanent Magnet Synchronous Generator for Ocean Wave Energy Conversion," *IEEE Transactions on Applied Superconductivity*, vol. 30, no. 4, pp. 1-4, June 2020. [Article \(CrossRef Link\)](#)
- [16] Y. Huo, X. Dong and S. Beatty, "Cellular Communications in Ocean Waves for Maritime Internet of Things," *IEEE Internet of Things Journal*, vol. 7, no. 10, pp. 9965-9979, Oct. 2020. [Article \(CrossRef Link\)](#)
- [17] S. Borade, L. Zheng and R. Gallager, "Amplify-and-Forward in Wireless Relay Networks: Rate, Diversity, and Network Size," *IEEE Transactions on Information Theory*, vol. 53, no. 10, pp. 3302-3318, Oct. 2007. [Article \(CrossRef Link\)](#).
- [18] Levin, George and Sergey L. Loyka. "Amplify-and-forward versus decode-and-forward relaying: which is better?," in *Proc. of The 22nd International Zurich Seminar on Communications (IZS)*, pp. 123-125, March 2012. [Article \(CrossRef Link\)](#)



**Kyeongjea Lee** received the B.S. degrees from the School of Electronic Engineering, Gachon, Gyeonggi, South Korea, in 2018. He is currently working toward the Ph.D. degree at the Electrical and Electronic Engineering, Yonsei University, Seoul, South Korea. His research interests include the advanced MIMO technologies for wireless communication systems.



**Tae-Woo Kim** received the B.S. degrees from the School of Electrical and Electronic Engineering, Yonsei University, Seoul, South Korea, in 2015, where he is currently pursuing the Ph.D. degree. His research interests are wireless communication systems.



**Sungyoon Cho** received the B.S., M. S. and Ph.D. degrees in electrical and electronic engineering from Yonsei University, Seoul, Korea, in 2006, 2008, and 2013, respectively. From 2013 to 2020, he was with Samsung Electronics, Korea, as a Staff Engineer to research cellular communication systems and develop 4G and 5G modem chipset. Since 2020, he has been with Korea Electronics Technology Institute (KETI) as a Principal Researcher to develop the advanced technologies for embedded network. His research interests are in the fundamental aspects of wireless communication and signal processing and learning algorithms for practical application.



**Kiwon Kwon** received B.S. and M.S. degrees in computer engineering from Kwangwoon University, Korea, in 1997 and 1999, He also received the Ph.D. degree in the School of Electrical & Electronics Engineering from Chung-Ang University, Korea, in 2011. In 1999, he joined in KETI, Korea, where he is currently a Group Leader with Oceans and Fisheries ICT Group. His research interests are in the area of advanced broadcasting/communication system, digital twin, oceans and fisheries ICT.



**Dong Ku Kim** (Senior Member, IEEE) has been a professor at the School of Electrical and Electronic Engineering, Yonsei University, since 1994. He is a chair of the governing board of the public-private Open RAN Industry Alliance in Korea. He is also a member of the special committee for national strategic technology under the presidential advisory council on S&T. He served as a chair of the public-private 5G Forum executive committee over the last ten years and a member of the 5G+ strategy committee chaired by the minister of the Ministry of Science and ICT minister (MSIT). He received the Yellow Stripes of the Order of Service Merit from the Korean government for the contribution of the world's first commercialization of 5G, ecosystem creation, and the defusion of convergence among 5G-based industries in April 2020. He received IEEE Communication Society Career Award for Public Service in the Field of Telecommunication on Dec.2020. He received his Ph.D. from the University of Southern California, Los Angeles, in 1992. He worked on CDMA systems in the cellular infrastructure group of Motorola at Fort Worth, Texas. His current research interests are the advanced MIMO for 5G vehicular use cases, RSMA for future mobile systems, smart buoy energy efficient transmission, and Open RAN.